Ferrimagnetic glass ceramics nanoparticles produced by high-energy ball milling technique

Nehal A. Erfan [1*], Ibrahim Hamed M. Aly [1], Salwa A. M. Abdel-Hameed [2], Barbara J. Muller-Borer [3]

Abstract: In the present study soft ferrimagnetic glass ceramic nanoparticles (MNPs) were prepared by high energy mechanical ball milling utilizing a planetary ball mill. Various MNPs samples were produced by changing the milling time from 1h to 5h, in the constant milling speed of 1200 rpm. Transmission electron microscopy (TEM) and vibrating sample magnetometer (VSM) analysis were performed to determine the characteristics of primary (unmilled) and milled samples. Using high energy planetary ball milling technique, nanoparticles with a very narrow particle size distribution and uniform spherical shaped morphology were obtained. The average particle size reached after 5 hours milling was 10 nm. Moreover, it was found that the saturation magnetization decreased with increasing milling time. The coercivity decreased and after that increased to reach 88 Oe after 5 hours milling.

Key Words: Magnetic glass ceramics, Ball milling, Magnetic nanoparticles and freeze drying technique

[1] **Faculty of engineering, Minia university, Egypt**

[2] **Glass department, National research center, Doki, Cairo, Egypt**

[3] **Department of Engineering, East Carolina University, Greenville, NC, USA.**

*Corresponding author

E-mail: nehalerfan@yahoo.com

1. Introduction

Owing to the growing amount of solid waste produced by industrial firms and the enforced environmental regulations as well as the needs to pollution abatement, an increasing interest has been developed to utilize recycling as a means of diverting solid wastes into new glass-ceramic products. Iron ore is upgraded to a higher iron content through concentration, the concentrate must be pelletized in order to feed a blast furnace or a DRI plant. Pellets are indurated, spheres of ore with a high iron content and uniform quality. Huge amount of broken pellets (up to 8% of pellets burden) are wasted annually during travelling process from Brazil to Egypt, so reducing the environmental impact of broken pellets will give its product further important benefits and offer a significant potential for cost savings profit if reintroduced into the industrial process through well planned programs. Glass-ceramics are defined as composite material that contains at least one crystalline phase dispersed in an amorphous glassy matrix. Composites containing dispersed magnetic particles in a glass matrix are important

materials for developing compact glass ceramic and glass coated magnetic particles.

One-dimensional magnetic nanostructures have recently attracted much attention because of their intriguing properties that are not displayed by their bulk or particle counterparts. These nanostructures are also potentially useful as active components for ultrahigh- density data storage, as well as in the fabrication of sensors and spintronic devices [T. Thurn-Albrecht et. al., 2000; D. A. Allwood et. al., 2002; J. I. Martı´n et. al., 2003; A. Fert and L. Piraux, 1999] [1-4]. For example, nanoscale magnetic logic junctions have recently been fabricated with ferromagnetic nanowires as building blocks [D. A. Allwood et. al., 2002] [2]. In addition, nanostructured magnetic materials have unique properties and potential applications in catalysis [A.H. Lu, W. Schmidt et. al., 2004] [5], biotechnology/biomedicine [A.K. Gupta and M. Gupta, 2005; Z. Li et. al., 2005] [6,7], magnetic resonance imaging (MRI) [L. Babes et. al., 1999] [8], magnetic fluids [V. Socoliuc et. al., 2003] [9], high density information storage [S.H. Sun et. al., 2000][10] and magnetooptical devices [G. Shemer and G. Markovich, 2002] [11]. Developing new and, in particular, cost effective techniques for fabricating ferrite nanostructures is of great scientific and commercial interest. Co-precipitation [Fun

Chin, Suk et.. al., 2008; Nigel Smith et. al.] [12,13], thermal decomposition [A.-H. Lu et. al., 2007][14], microemulsion [S S.Rana et. al., 2010; E. K. Athanassiouet. Al., 2010] [15,16], and flame spray [R. N. Grass et. al., 2006; El-Eskandarany MS, 2001][17,18] synthesis are the most common chemical procedures for nanoferrite preparation. There are several disadvantages to these techniques such as complicated synthesis schemes and equipment, high costs of reactants, long production cycle and low material yield. Therefore, there is a demand for an alternative synthesis technique, which is simple, reliable, environmental friendly and cost-effective for large-scale production of nano-ferrites. Within top-down technologies, one of the most representative techniques is high-energy ball milling (HEBM). This technique is well-known as a simple and inexpensive method for production of nano-structured materials [A.-H. Lu et. al., 2007][14]. In HEMB, particles of starting material are subject to heavy deformation, cold work-hardening and subsequent fragmentation. This work aims to study the possibility of converting ferrimagnetic glass ceramics into magnetic nanoparticles using high energy ball milling technique i.e. top-down technique. The produced nano-magnetic glass ceramics can be used in different applications.

2. Experimental Methods

The detailed preparation methodology of the magnetic glass ceramic precursor was discussed in a previous work **[19] (**Salwa A.M. Abdel-Hameed et. al., 2014**).**

2.1 Preparation of the magnetic glass ceramic precursor

XRF analysis of BPW sample is illustrated in Table 1. Ferrimagnetic glass ceramicswere prepared based on crystallization of $ZnFe_2O_4$ as soft magnet. The composition of prepared samples is shown in Table 2. Soft magnetic glass ceramics (SMGC) sample contain about 54% of the broken pellets waste.

A small amount of ZnO as $ZnCO_3$, Na_2O as Na_2CO_3, P_2O_5 as $NH_4H_2PO_4$, TiO_2, and B_2O_3 as H3BO3 were added to complete the design of desired phases. The samples were prepared by melting the required amounts of reagent grade with the composition shown in Table 2 in platinum crucibles at about 1500˚C for 2 hours, in an electrically heated furnace with occasional swirling every 30 minutes to ensure homogenization. The melts were poured on to a stainless steel plate at room temperature and pressed into 1-2 mm thick strips by another cold steel plate.

For this study two grinding methods to produce nanoparticles from the magnetic glas ceramic samples were evaluated: hand ground with an agate mortar and high energy ball-milling procedure.

Table1: Quantitative XRF analysis of broken pellets waste (BPW).

Main Constituents	(wt,%)
SiO_2	2.31
TiO_2	0.08
Al_2O_3	0.97
$Fe_2O_3^{tot.}$	95.06
MgO	0.08
CaO	0.98
Na_2O	0.06
K_2O	0.02
P_2O_5	0.11
CuO	0.043
Cr_2O_3	0.069
MnO	0.002
SO3	0.05
LOI	0.12
Cl	0.042

Table 2: Chemical composition in wt% of the prepared magnetic glass ceramics

Compound	Chemical Composition wt%
Fe2O3	**65.5**
SiO2	**-**
TiO2	**0.005**
ZnO	**1.6**
Al2O3	**0.67**
MgO	**0.055**
CaO	**0.675**
Na2O	**0.04**
K2O	**0.014**
P2O5	**4.21**
CuO	**0.03**
Cr2O3	**0.05**
MnO	**0.138**
B2O5	**22.66**
BaO	**-**

2.2 preparation of the magnetic glass ceramic nano particles

High- energy ball milling was carried out at room temperature using VQ-N Desktop high speed vibrating ball mill (Figure 1). One end of the principal axis of the mill connects with an eccentric wheel which is connected with the foundation of the ball mill through a tensile spring. When in operation the eccentric wheel swings at a high speed due to the tension of the spring. With the powerful vibration generated by the high speed swinging of the eccentric wheel, the ball milling jars fixed on the eccentric wheel rotate and vibrate at 1200 rpm. A zirconium oxide jar (Figure 2) was used with a stainless steel vacuum cover during the milling process in vacuum environment. Granularity of the material specimens placed in the jar was less than 1mm and the maximum material loading was two thirds of the cubage of the ball milling jar (including milling balls). Two Zirconium oxide balls of 20 mm diameter were used in milling process. The material was processed for 1, 3 or5 h), at the end of the milling time , samples were collected

Figure 1 : VQ-N Desktop high speed vibrating ball mill (purchased from Across international Livingston, United States)

Figure 2: Ball mill accessories: Stainless steel vacuum jar, ceramic & stainless steel jar, stainless steel & ceramic grinding balls.

2.3 Sample Preparation For TEM Imaging

Sample preparation in TEM can be a complex procedure. [Cheville, NFand Stasko J, 2014] **[20]** TEM specimens are required to be at most hundreds of nanometers thick, as unlike neutron or X-Ray radiation the electron beam interacts readily with the sample, an effect that increases roughly with atomic number squared (z^2). [Fultz, B and Howe, J, 2007] **[21]** High quality samples will have a thickness that is comparable to the mean free path of the electrons that travel through the samples, which may be only a few tens of nanometers. Preparation of TEM specimens is specific to the material under analysis and the desired information to obtain from the specimen. Materials that have dimensions small enough to be electron transparent, such as powders or nanotubes, can be quickly prepared by the deposition of a dilute sample containing the specimen onto support grids or films. Applying usual preparation methodology on the ball milled samples under investigation resulted in not evenly distributed particles on the formvar grid but rather were on the grid bars so therefore unobservable in the TEM (Figure 6). As such, we had to look for alternative technique to enable imaging the nanoparticles.

(a)

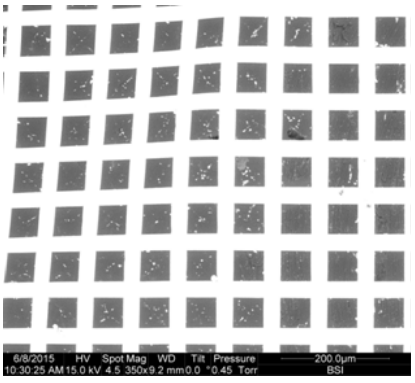

(b)

Figure 3, TEM grid (a)after usual air drying preparation of the sample, (b) SEM image after freeze drying technique

A freeze- drying technique was used o improve the long-term stability of colloidal nanoparticles [F. Franks, 1998]**[22]** and enable successful imaging under the TEM.

Freeze-drying, also known as lyophilization , is a process of removing water from a frozen sample by sublimation and desorption under vacuum. With this technique, specimens can have a shelf life of several years [D. Quintanar-Guerrero et. al., 1998; W. Abdelwahed et. al., 2006; W. Abdelwahed et. al., 2006]**[23-25]**. The freeze drying cycle can be divided into three steps: freezing (solidification), primary drying (ice sublimation) and secondary drying (desorption of unfrozen water).

3. Freezing step

It is the first step of freeze drying. During this step, the liquid suspension is cooled, and ice crystals of pure water forms. As the freezing process continues, more and more water contained in the liquid freezes. This results in increasing concentration of the remaining liquid. As the liquid suspension becomes more concentrated, its viscosity increases inducing inhibition of further crystallization. This highly concentrated and viscous liquid solidifies, yielding an amorphous, crystalline, or combined amorphous-crystalline phase [F. Franks, 1990] **[26]**. The small percentage of water that remains in the liquid state that does not freeze is called bound water.

Primary drying step

The primary drying stage involves sublimation of ice from the frozen product. In this process, i) heat is transferred from the shelf of the frozen solution through the tray and vial, and conducted to the sublimation front, ii) the ice sublimes and the water vapor formed passed through the dried portion of the product to the surface of the sample, iii) the water vapor is transferred from the surface of the product through the chamber to the condenser, and iv) the water vapor condenses on the condenser. At the end of sublimation step a porous plug is formed. Its pores correspond to the spaces that were occupied by ice crystals [N.A. Williams and G.P. Polli, 1984]**[27].**

4. Secondary drying

Secondary drying involves the removal of absorbed water from the product. This is the water which did not separate out as ice during the freezing, and did not sublimate off [M.J. Pikal et. al., 1990]**[28].**

Figure 7 shows the Labcono apparatus used for the SMGC nanoparticles freeze drying; it consists of drying chamber containing temperature-controlled shelves, which is connected to a condenser chamber. The condenser chamber houses of coils capable of being maintained at very low temperature (less than -50). Vacuum pump is connected to the condenser chamber to achieve pressure in the range of 4 to 40 Pa in the entire system during operation [M.J. Pikal, 2002]**[29]**.

Figure 4, LABCONO freeze dryer

5. Characterization

The morphological study for the precursor material and for the nanoparticles was carried out with a transmission electron microscope (TEM 2010). Magnetic properties were evaluated using vibrating sample magnetometer (Quantum Design(R), Magnetic Property Measurement System (MPMS), SQUID VSM).

6. Results and discussions

Figure 5 represents TEM images of the nanoparticles prepared by milling SMGC powder for different 1,3 and 5 h. There was no significant change in morphology of the nanoparticles with increase in milling time up to 5 h. Figure 5(a) shows a wide particle size distribution from (2-4 μ m) with a significant particles agglomeration after 1 h milling time. Figure 5(b), shows uniform spherical shaped particles with mean particle size of 2 μm with some agglomeration. Figure 5(c) clearly shows that after 5 h milling a very narrow size distribution and ultrafine particle sizes of 10 nm average diameter. The nanoparticles can self-assemble into a regular pattern which is achieved by the freeze drying technique. There is a distinguishable difference in the micro-structure regarding particle shape and particle size distribution of SMGC particles, obtained from hand grinding and planetary ball milling. The difference of reactivity is considered to be the dominant reason for this variablitliy.. With planetary ball milling, the reactants connect directly with higher probability and react adequately for the higher energy from the ball collisions [Zhigang Zhang et. al., 2015]**[30]**. The reason for the absence of elongated structures in nanoparticles after 5 hours milling can be due to the body centered cubic structure (bcc) of Fe and $FeZn_2O_4$ (V. M. Chakka et. al., 2006)**[31]**. Materials with hexagonal and tetragonal structures have a preferred orientation for fracture which are the hexagonal closed packed planes [(0001) for hcp], and form plate-like structures [G. E. Dieter, 1988] **[32]**, which upon further milling would result in the formation of elongated structures.

This result is consistent with [V. M. Chakka et. al., 2006] **[31]**work as they prepared nanoparticles of Fe, Co, FeCO, SmCO, and NdFeB with sizes smaller than 30 nm by ball milling in the presence of surfactants and organic carrier liquid.

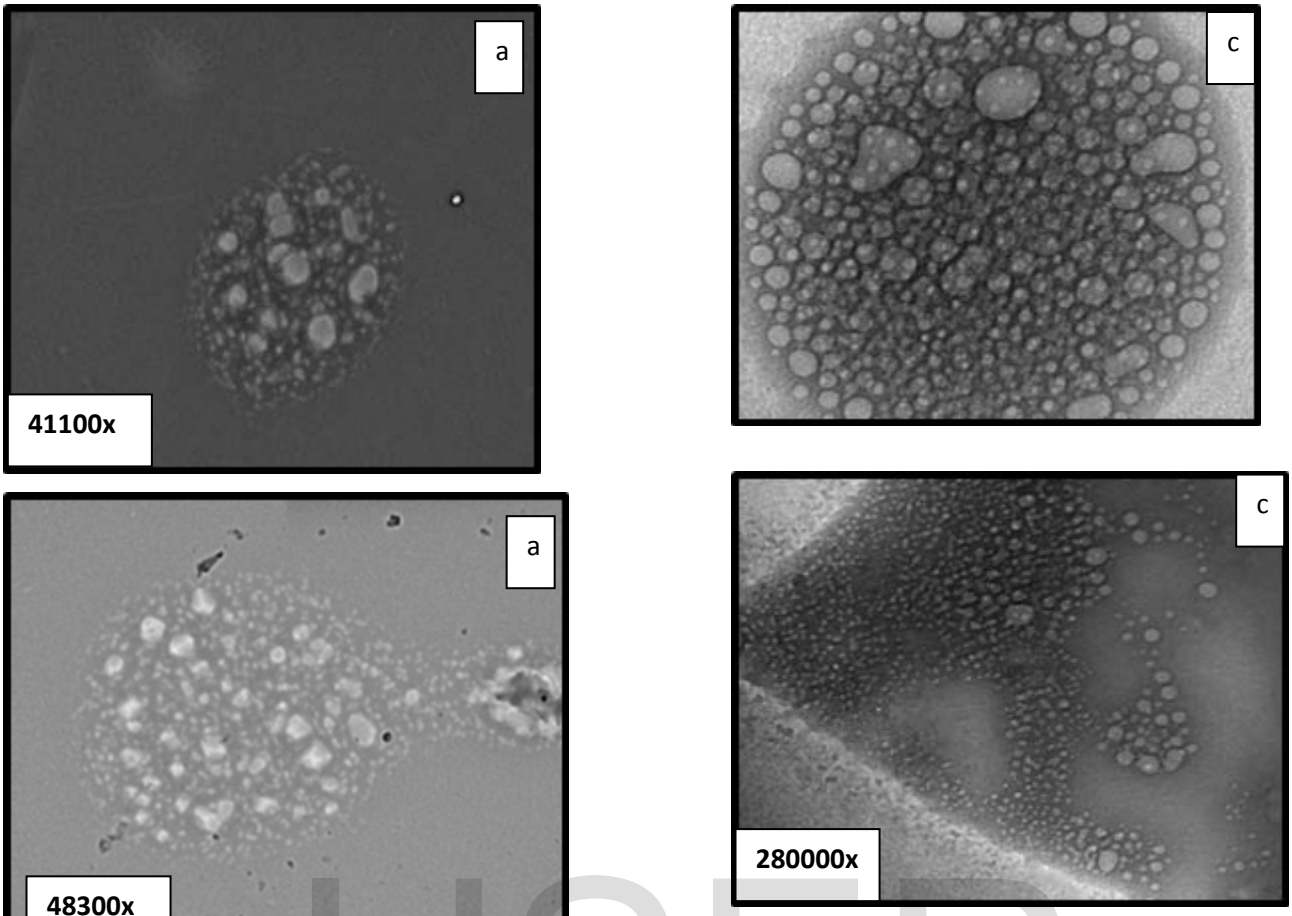

Figure (5), TEM images of **(a)** 1hr, **(b)** 3hrs, and **(c)** 5hrs milling time at different magnifications and locations of the TEM grid.

Figure 6a shows the room temperature magnetic hysteresis (*M-H*) loops of hand milled MGC and the particles after 1, 3 and 5 hours milling time under a magnetic field strength of 20 kOe. Figure 6b represents the effect of milling time on saturation magnetization and coercivity. Table 3 displays the relevant magnetic parameters: saturation magnetization (*Ms*), remanence (*Mr*), Coercivity (*Hc*) and *Mr*/*Ms* ratio obtained from *M-H* loops. In general the magnetic field necessary to saturate the samples increases with Zn-ferrite crystallization increase. Figure 6

demonstrates that, Ms decreased by increasing milling time to reach 53 emu/g after 5 hours milling. As expected, saturation magnetization is directly proportional to the degree and amount of crystallization of Zn-ferrite. It should be considered that Zn-ferrite is a ferromagnetic phase and amorphous glass matrix is an antiferromagnetic material with a very low saturation magnetization. As a consequence, the variation of the saturation magnetization can be attributed to the modification of the quantity of Zn-ferrite crystals (Roy MK et. al., 2006) **[32]** present in the glass ceramic samples. The coercivity decreased from 26 Oe for hand milled sample to 5 Oe after 1 hour milling and after that kept increasing by increasing milling time to reach the maximum value 88 Oe after 5 hours milling. Large saturation magnetization usually values have been correlated with the high crystallinity of the nanoparticles (S. Chkoundali et. al., 2004) **[33]** as well as defects such as cation redistribution, the existence of surface spins, formation of spin glass structures and the presence of ZnO. The coercivity has been affected by the grain size, defects presence, strains, magnetocrystalline anisotropy, shape anisotropy and surface disorder (A. B. Nawale et. al., 2011) **[34]**. The defects and strains presence, derived from the continual ball collisions with high energy in the planetary ball milling process, is accounted primarily for the difference in magnetic properties of MGC powder after different milling time. In the grinding by hand process, the reactants, only in the interaction region of the mortar and pestle, can be ground to a limited extent. In the planetary ball milling process, almost all of the reactants are in the interaction region of the balls so that they can be simultaneously ground. The strains and defects generated by the innumerable high energy ball collisions, are still abound in the products. These findings explain the sharp decrease in Hc after 1 hour milling and the subsequent increase by increasing milling time (Figure 6b). In the case of nanoparticles prepared by milling the MGC powder for 5 hours, superparamagnetic behavior was observed at room temperature. Magnetic measurements at room temperature showed some hysteresis with coercivities up to 88 Oe, and saturated loop from 5 KOe, implying a combination of superparamagnetic and ferromagnetic behavior at 300 K. Magnetic properties of the nanoparticles prepared by milling MGC powders showed hysteresis at room temperature with low coercivity (<100 Oe) and very low remenance ratio (*Mr/Ms*) of less than 0.1. It can be observed from the loops that *Mr/Ms* values increased from 0.03 form the hand milled to 0.08 after 5 h milling. This remanence ratio enhancement could be due to the increasing percentage of fractured particles and higher aspect ratios for longer milling time or the formation of most of the nanoparticles rather than the

disordered boundary regions with increasing milling time (V. M. Chakka, B. Altuncevahir et. al.,2006) **[31].**

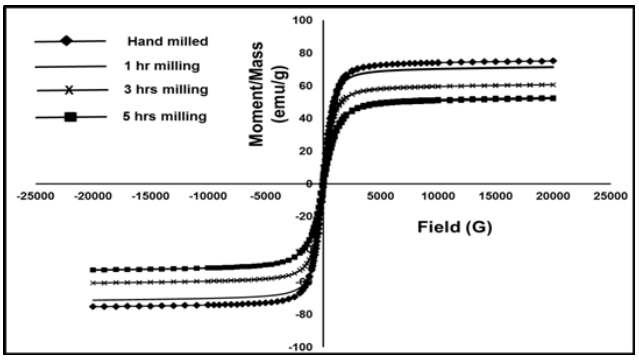

(a)

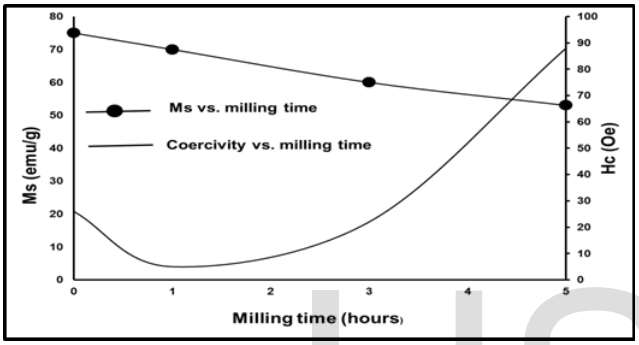

(b)

Figure (6), (a) Magnetization curves of hand milled, 1hr, 3 hrs and 5 hrs milling time PS, **(b)** Effect of milling time on saturation magnetization and coercivity.

Table (3), Magnetic properties of hand milled, 1hr, 3hrs, and 5 hrs milling particles.

Sample	Ms (emu/g)	Mr (emu/g)	Hc (Oe)	Mr/Ms
Hand milled	75	2.5	26	0.033
1 hr milling	70	0.5	5	0.007
3 hrs milling	60	1.5	22	0.025
5 hrs milling	53	4.32	88	0.082

5. Conclusions

1- Using mechanical milling technique, SMGC sample with (10±1.92) nm average particle size has been obtained after 5 hours milling time.

2- The produced nanoparticles after 5 hours milling, have the same features and elemental composition of the starting sample precursor. This result has been confirmed using TEM .

3- The effect of mechanical milling on the SMGC properties can be concluded as follows:.

- Saturation magnetization decreased by increasing milling time to reach 53 emu/g at 5 hours.
- The sample coercivity decreased to 5 Oe at 1 hour milling, and after that kept increasing proportionally by increasing milling time to reach 88 Oe at 5 hours.

4- The prepared nanoparticles using the ball milling technique can be used in ferrofluid technology, magnetic nanofibers preparation and waste water treatment applications.

ACKNOWLEDGMENT

This work was supported financially by the Science and Technology Development Fund, STDF (1024).

References

[1] T. Thurn-Albrecht, J. Schotter, G. A. Ka¨stle, N. EmLey, T. Shibauchi, L. Krusin-Elbaum, K. Guarini, C. T. Black, M. T. Tuominen, and T. P. Russell, Ultrahigh-density nanowire arrays grown in self-assembled diblock copolymer templates. Sience, 290 (2000) 2126.

[2] D. A. Allwood, G. Xiong, M. D. Cooke, C. C. Faulkner, D. Atkinson, N. Vernier, and R. P. Cowburn, Submicrometer Ferromagnetic NOT Gate and Shift Register. Science, 296 (2002) 2003.

[3] J. I. Martı´n, J. Nogue´s, K. Liu, J. L. Vicent, and I. K. Schuller, Ordered magnetic nanostructures: fabrication and properties. J. Magn. Magn. Mater., 256 (2003) 449.

[4] A.H. Lu, W. Schmidt, N. Matoussevitch, H. Bönnemann, B. Spliethoff, B. Tesche, E. Bill, W. Kiefer, F. Schüth, Nanoengineering of a magnetically separable hydrogenation catalyst. Chem. Int. Ed., 43 (2004) 4303

[5] A.K. Gupta, M. Gupta, Synthesis and surface engineering of iron oxide nanoparticles for biomedical applications. Biomaterials, 26 (2005)3995.

[6] Z. Li, L. Wei, M.Y. Gao, H. Lei, One-pot reaction to synthesize biocompatible magnetite nanoparticles, Adv. Mater. 17 (2005) 1001–1005.

[7] L. Babes, B. Denizot, G. Tanguy, J.J.L. Jeune, P. Jallet, Synthesis of Iron Oxide Nanoparticles Used as MRI Contrast Agents: A Parametric Study. J. Colloid Interface Sci. ,212 (1999) 474.

[8] V. Socoliuc, D. Bica, L. Vekas, Estimation of magnetic particle clustering in magnetic fluids from static magnetization experiments. J. Colloid Interface Sci., 264 (2003) 141

[9] S.H. Sun, C.B. Murray, D. Weller, L. Folks, A. Moser, Monodisperse FePt nanoparticles and ferromagnetic FePt nanocrystal superlattices, Nature 287 (2000) 1989–1992.

[10] G. Shemer, G. Markovich, Enhancement of Magneto-Optical Effects in Magnetite Nanocrystals Near Gold Surfaces. J. Phys. Chem. B , 106 (2002) 9195

[11] Suk Fun Chin, K. Swaminathan Lyer, Colin L. Raston, Martin Saunders, Size Selective Synthesis of Superparamagnetic Nanoparticles in Thin Fluids under Continuous Flow Conditions. Advanced functional materials, 18(2008)922.

[12] Nigel Smith, Colin L. Raston, Martin Saunders, Robert Woodward, synthesis of magnetic nanoparticles using spinning disc processing. NSTI-Nanotech, 1(2006)343.

[13] A.-H. Lu, E. L. Salabas and F. Schüth,. Angew., Magnetic Nanoparticles: Synthesis, Protection, Functionalization, and Application. Chem. Int., 46(2007)1222.

[14] S S.Rana, J. Philip, B.Raj, Micelle based synthesis of cobalt ferrite nanoparticles and its characterization using Fourier Transform Infrared Transmission Spectrometry and Thermogravimetry. Materials Chemistry and Physics, 124(2010)264.

[15] E. K. Athanassiou, Evagelos K.; R. N. Grass; W. J. Stark, Chemical Aerosol Engineering as a Novel Tool for Material Science: From Oxides to Salt and Metal Nanoparticles. Aerosol. Sci. Tech., **44**(2010)161.

[16] R. N. Grass, Robert N.; W. J. Stark, Gas phase synthesis of fcc-cobalt nanoparticles. J. Mater. Chem., **16**

(2006) 1825.

[17] El-Eskandarany MS, Mechanical allying for fabrication of advanced engineering materials. Norwich, New York, William Andrew Publishing, (2001).

[18] Donya Ramimoghadam, Samira Bagheri and Sherifah Bee Abd Hamid, Stable monodisperse nanomagnetic colloidal suspensions. Colloids and surfaces B: Biointerfaces, 133 (2015) 388.

[19] Salwa A. M. Abdel-Hameed, Ibrahim M. Hamed, Nehal A. Erfan, Utilization of iron oxide bearing pellets waste for preparing hard and soft ferromagnetic glass ceramics . Journal of advanced ceramics, 3 (2014) 259.

[20] Cheville, NF and Stasko J, Techniques in Electron Microscopy of Animal Tissue. Veterinary Pathology, 51(2014)28.

[21] Fultz, B and Howe, J, Transmission Electron Microscopy and Diffractometry of Materials, 4th edititon. Springer, (2007).

[22] F. Franks, Freeze-drying of bioproducts: putting principles into practice. Eur. J. Pharm. Biopharm., 45(1998)221.

[23] D. Quintanar-Guerrero, A. Ganem-Quintanar, E. Allémann, H. Fessi, E. Doelker, Influence of the stabilizer coating layer on the purification and freeze-drying of poly (D,L-lactic acid) nanoparticles prepared by an emulsion–diffusion technique. J. Microencapsul, 15(1998)107.

[24] W. Abdelwahed, G. Degobert, H. Fessi, Investigation of nanocapsules stabilization by amorphous excipients during freeze-drying and storage. Eur. J. Pharm. Biopharm., 63(2006)87.

[25] W. Abdelwahed, G. Degobert, H. Fessi, A pilot study of freeze drying of poly(epsiloncaprolactone) nanocapsules stabilized by poly(vinyl alcohol): formulation and process optimization. Int. J. Pharm., 17 (2006)178.

[26] F. Franks, Freeze-drying: from empiricism to predictability. Cryo-lett. 11 (1990) 93.

[27] N.A. Williams, G.P. Polli, The lyophilization of pharmaceuticals: a literature review. J. Parenter. Sci. Technol., 38 (1984)48.

[28] M.J. Pikal, S. Shah, M.L. Roy, R. Putman, The secondary drying stage of freeze-drying: drying kinetics as a function of temperature and chamber pressure. Int. J. Pharm., 60 (1990)203

[29] M.J. Pikal, Freeze drying, in: J. Swarbrick (Ed.), Encyclopedia of Pharmaceutical Technology, vol. 2, Marcel Dekker, New York, (2002).

[30] Zhigang Zhang, Guangchun Yao, Xiao Zhang, Junfei Ma, and Hao Lin, Synthesis and characterization of nickel ferrite nanoparticles via planetary ball milling assisted solid-state reaction. Ceramics international, 41(2015) 4523.

[31] V. M. Chakka, B. Altuncevahir, Z. Q. Jin, Y. Li, and J. P. Liu, Magnetic nanoparticles produced by surfactant-assisted ball milling. Journal of applied physics, 99(2006)08E912-1.

[32] M. K. Roy, B. Haldar, H. C. Verma, Characteristic length scales of nanosize zinc ferrite. Nanotechnology, 17(2006)232.

[33] S. Chkoundali, S. Ammar, N. Jouini, F. Fiévet, P. Molinié, M. Danot, F. Vallain, J. M. Grenèche, Nickel ferrite nanoparticles: elaboration in polyol medium via hydrolysis, and magnetic properties. J. Phys.: Condens. Matter, 16(2004)4357.

[34] A.B. Nawale, N. S. Kanhe, K. R. Patil, S. V. Bhoraskar, V. L. Mathe, A. K. Das, Magnetic properties of thermal plasma synthesized nanocrystal- line nickel ferrite (NiFe2O4), J. Alloy. Compd., 509(2011)4404.